Ion transfer and adsorption behavior of ionizable drugs affected by PAMAM dendrimers at the water|1,2- dichloroethane interface

Ion transfer and adsorption behavior of ionizable drugs affected by PAMAM dendrimers at the water|1,2-dichloroethane interface

Hiroki Sakae[a], Hirohisa Nagatani[b,*,1] and Hisanori Imura[b]

[a] Division of Material Sciences, Graduate School of Natural Science and Technology, Kanazawa University, Kakuma, Kanazawa 920-1192, Japan

[b] Faculty of Chemistry, Institute of Science and Engineering, Kanazawa University, Kakuma, Kanazawa 920-1192, Japan

*Corresponding author: Hirohisa Nagatani

e-mail: nagatani@se.kanazawa-u.ac.jp

[1] ISE member

Abstract The transfer and adsorption reactions of ionizable drug molecules, i.e. dipyridamole (DIP), propranolol (PRO) and warfarin (WAR), at the water|1,2-dichloroehtane (DCE) interface were studied in the presence of the carboxylate-terminated generation 3.5 (G3.5) or amino-terminated generation 4 (G4) polyamidoamine (PAMAM) dendrimers. The ionic partition diagram of the ionizable drugs was determined through the voltammetric analysis of ion transfer responses. In the DIP system, the additional voltammetric responses associated with the interfacial adsorption were observed in the positive potential region. Although the spectroscopic features of the drug species in the aqueous solution were hardly affected by the addition of the dendrimers, the ion transfer currents in the DIP and PRO systems were decreased in the presence of the G3.5 PAMAM dendrimer indicating the intermolecular association between the cationic drugs and negatively charged dendrimers in the interfacial region. The interfacial mechanism of the fluorescent DIP species was investigated in detail by potential-modulated fluorescence (PMF) spectroscopy. The PMF results demonstrated that the monoprotonated form, $HDIP^+$, was transferred across the water|DCE interface accompanied by the adsorption process. The interfacial mechanism of the DIP species was significantly modified by the dendrimer, depending on the pH condition. Under acidic conditions, the positively charged G3.5 PAMAM dendrimer adsorbed at the interface effectively prevented the coadsorption of $HDIP^+$. At higher pHs, DIP (or $HDIP^+$) interacted with the hydrophobic interior moiety (or negatively charged periphery) of the dendrimers.

Keywords ionizable drug, interface between two immiscible electrolyte solutions (ITIES), ionic partition diagram, PAMAM dendrimer, potential-modulated fluorescence (PMF)

1. Introduction

Electrochemical approaches have been well established for studying the partition behavior of ions and ionizable compounds across the interface between two immiscible electrolyte solutions (ITIES) [1-3]. It is significantly important to determine the physicochemical properties of drugs in biomimetic liquid-liquid distribution systems since the pharmacokinetics of drugs involves heterogeneous charge transfer and adsorption processes on or across a biomembrane. The ionic partition diagram is one of the most important data to evaluate the distribution property of ionic species and it allows us to trace the transfer potential and distribution equilibria of ionic species as a function of pH [4]. In order to characterize pharmacological properties *in vivo*, a variety of drug molecules have been investigated at biomimetic liquid|liquid interfaces [5-10].

Dendrimers are unique and nontraditional polymers which have a number of advantages as drug carriers or containers [11-18]: well-defined three-dimensional structure with low polydispersity, bifunctional reactivity of interior and periphery moieties, biocompatibility and so on. Dendrimers have therefore attracted much attention to develop the drug delivery systems (DDS). The fundamental aspects of ion transfer reaction of dendritic species have been studied at the water|1,2-dichloroethane (DCE) interface [19-22]. The spectroelectrochemical analysis of charge transfer reactions elucidated the potential-driven encapsulation of anilinonaphthalenesulfonates in the carboxylate-terminated generation 3.5 (G3.5) polyamidoamine (PAMAM) dendrimer at the polarized water|DCE interface [23]. Recently, The ion association behavior of the amino-terminated PAMAM dendrimers with water-soluble porphyrins at the interface was also investigated in terms of dendritic generation, pH condition, effect of metal center and so on [24]. The PAMAM dendrimer-zinc(II) porphyrin associates showed a high photoreactivity in the heterogeneous photoinduced electron transfer system at the

water|DCE interface [25]. Although these interfacial characteristics of the charged dendrimer associated with ionic species imply its capability in DDS, the intermolecular interaction between the dendrimer and drug molecules has not yet been studied at ITIES.

In this study, we investigated the ion transfer reaction of ionizable drugs, i.e. dipyridamole (DIP), propranolol (PRO) and warfarin (WAR), affected by the PAMAM dendrimers at the water|DCE interface. The ionic partition property of cationic PRO and anionic WAR molecules as common drugs has been widely investigated at ITIES [5, 6, 9, 26]. Dipyridamole (DIP) is a well-known coronary vasodilator and a coactivator of antitumor compounds [27, 28], and its characteristics in aqueous solution have been studied through conventional spectroscopic measurements [29-31]. The interfacial properties of drugs were analyzed through the voltammetric and spectroelectrochemical measurements. The specific interaction between DIP and the dendrimer in the interfacial region was studied in detail by means of the potential-modulated fluorescence (PMF) spectroscopy.

2. Experimental

2.1. Reagents

The G3.5 and G4 PAMAM dendrimers with ethylenediamine core were purchased from Aldrich (10 wt% in methanol) and prepared as an aqueous solution after removing methanol by drying in ultrapure argon (> 99.999%). The molecular structures of ionizable drugs are shown in **Fig. 1**. Dipyridamole (DIP) (TCI > 98%), propranolol (PRO) (Aldrich > 99%) and warfarin (HWAR) (Nacalai Tesque > 98%) were used as received. The composition of the electrochemical cell is represented in **Fig. 2**. It should be noted that DIP was initially dissolved in the organic phase under the neutral and alkaline conditions because of its low solubility in water. The supporting

electrolytes were 1.0×10^{-2} mol dm^{-3} LiCl for the aqueous phase and 5.0×10^{-3} mol dm^{-3} bis(triphenylphosphoranylidene)ammonium tetrakis(pentafluorophenyl)borate (BTPPATPFB) for the organic phase, respectively. BTPPATPFB was prepared by metathesis of bis(triphenylphosphoranylidene)ammonium chloride (BTPPACl) (Aldrich > 97%) and lithium tetrakis(pentafluorophenyl)borate ethyl ether complex (TCI ≥ 70%). The organic solvent, 1,2-dichloroethane (DCE), was of HPLC grade (Nacalai Tesque > 99.7%). All other reagents were of the highest grade available. The aqueous solutions were prepared with purified water from a Milli-Q system (Millipore Direct-Q 3 UV). The pH of the aqueous phase was adjusted by the addition of HCl, 2.0×10^{-2} mol dm^{-3} LiH_2PO_4/LiOH, 2.0×10^{-2} mol dm^{-3} H_3BO_3/LiOH or LiOH.

2.2. Apparatus

The spectroelectrochemical cell used in all measurements was analogous to one reported previously [32]. The water|DCE interface with a geometrical area (S) of 0.50 cm^2 was polarized by a four-electrode potentiostat (Hokuto Denko HA1010mM1A). Platinum wires were used as counter electrodes in both aqueous and organic phases. The Luggin capillaries were provided for the reference electrodes (Ag/AgCl) in both phases. The Galvani potential difference ($\Delta_o^w\phi \equiv \phi^w - \phi^o$) was estimated by taking the formal transfer potential ($\Delta_o^w\phi^\circ$) of tetramethylammonium as 0.160 V [33]. The fluorescence spectra of the aqueous solution were measured by a fluorescence spectrophotometer (Hitachi F-2500).

2.3. Potential-modulated fluorescence spectroscopy

The water|DCE interface under electrochemical control was illuminated from the organic phase by a cw laser diode of 10 mW at 404 nm (Coherent CUBE 405-50C) under total internal

reflection (TIR). The angle of incidence to the interface (Ψ) was set as ca. 75°. The fluorescence emitted from the interfacial region was collected perpendicularly to the interface by an optical fiber fitted to a photomultiplier tube through a monochromator (Shimadzu SPG-120S). The ac modulated fluorescence signal was analyzed as a function of ac potential modulation at 1 Hz by a digital lock-in amplifier (NF LI5640). The potential sweep rate was 5 mV s^{-1}. Further details of the PMF setup and analytical procedure are described elsewhere [32, 34, 35]. All of the experiments were carried out in a thermostated room at 298 ± 2 K.

3. Results and Discussion

3.1. Ion partitioning of ionizable drugs in the water|DCE system

The intrinsic ion transfer reactions of basic (DIP and PRO) and acidic drug (HWAR) molecules were preliminary investigated by cyclic voltammetry and admittance measurements in the absence of the dendrimer. Typical cyclic voltammograms (CVs) and ac voltammograms (ACVs) measured for DIP under various pH conditions are shown in **Fig 3**. The apparent ion transfer potential of the cationic DIP species was determined from the half-wave potential ($\Delta_o^w\phi^{1/2}$) in CVs and the peak potential of admittance in ACVs, in which the $\Delta_o^w\phi^{1/2}$ value was shifted toward positive potentials with increasing pH. For example, the $\Delta_o^w\phi^{1/2}$ values observed through the admittance measurements at pH 2.0, 7.0 and 9.1 were 0.02 V, 0.15 V and 0.28 V, respectively. At pH 7.1, an additional positive voltammetric response was found around 0.30 V and this post-transfer response could be associated with the interfacial adsorption of cationic DIP species. The peak to peak separation for the transfer responses was 0.059 V at [DIP] = 1.0×10^{-5} mol dm^{-3} in agreement with the theoretical value for a monocationic species though slightly larger value (ca.

0.07 V) was observed at [DIP] = 8.0×10^{-5} mol dm^{-3} because of the partial overlap with the post-transfer adsorption response. The peak current was almost proportional to the square root of the potential sweep rate ($v^{1/2}$) for a quasi-reversible transfer of monocationic species. The voltammetric results indicated that the ion transfer of the monoprotonated form, $HDIP^+$, takes place dominantly through the diffusion controlled process.

The Nernst equation for the ion transfer of monobasic species, $HDIP^+$, is defined by [4, 36]:

$$\Delta_o^w\phi = \Delta_o^w\phi^{\circ'}_{HDIP^+} + \frac{2.303RT}{F}\log\frac{[HDIP^+]_o}{[HDIP^+]_w} \quad (1)$$

where $\Delta_o^w\phi^{\circ'}_{HDIP^+}$ is the formal ion transfer potential. When the concentrations of $HDIP^+$ in the aqueous and organic phases are equal to each other, the term $\log\left([HDIP^+]_o/[HDIP^+]_w\right)$ is zero in Eq. (1) and then the Nernst equation is simplified into:

$$\Delta_o^w\phi = \Delta_o^w\phi^{\circ'}_{HDIP^+} \quad (2)$$

The acid-base equilibrium between $HDIP^+$ in the aqueous phase and DIP in the organic phase is described as:

$$DIP_o + H_2O \rightleftharpoons HDIP^+_w + OH^- \quad (3)$$

When the spontaneous distribution of the neutral DIP occurs in the water|DCE system, the acidity constant of DIP in water ($K_{a,HDIP^+}$) can be expressed as a function of pH and the partition coefficient of the neutral DIP (P_{DIP}):

$$K_{a,HDIP^+} = \frac{[DIP]_w[H^+]_w}{[HDIP^+]_w} = \frac{[DIP]_o}{[HDIP^+]_w}\frac{[H^+]_w}{P_{DIP}} \quad (4)$$

$$pK_{a,HDIP^+} = -\log\left(\frac{[DIP]_o}{[HDIP^+]_w}\right) + pH + \log P_{DIP} \quad (5)$$

where P_{DIP} is identical to $[\mathrm{DIP}]_{\mathrm{o}}/[\mathrm{DIP}]_{\mathrm{w}}$ under dilute conditions. The equiconcentration boundary line of $\mathrm{HDIP}^{+}_{\mathrm{w}}$ and $\mathrm{DIP}_{\mathrm{o}}$ is given by:

$$\mathrm{pH} = \mathrm{p}K_{\mathrm{a,HDIP^+}} - \log P_{\mathrm{DIP}} \tag{6}$$

On the other hand, the boundary line of $\mathrm{HDIP}^{+}_{\mathrm{o}}$ and $\mathrm{DIP}_{\mathrm{o}}$ is derived from Eqs. (1) and (4):

$$\Delta^{\mathrm{w}}_{\mathrm{o}}\phi = \Delta^{\mathrm{w}}_{\mathrm{o}}\phi^{\circ'}_{\mathrm{HDIP^+}} + \frac{2.303RT}{F}\log\left(\frac{[\mathrm{HDIP}^+]_{\mathrm{o}}}{[\mathrm{DIP}]_{\mathrm{o}}}\right) + \frac{2.303RT}{F}\log\left(\frac{P_{\mathrm{DIP}}K_{\mathrm{a,HDIP^+}}}{[\mathrm{H}^+]_{\mathrm{w}}}\right) \tag{7}$$

In the case of equiconcentration of $\mathrm{HDIP}^{+}_{\mathrm{o}}$ and $\mathrm{DIP}_{\mathrm{o}}$, Eq. (7) can be rewritten as:

$$\Delta^{\mathrm{w}}_{\mathrm{o}}\phi = \Delta^{\mathrm{w}}_{\mathrm{o}}\phi^{\circ'}_{\mathrm{HDIP^+}} + \frac{2.303RT}{F}\left(\log P_{\mathrm{DIP}} - \mathrm{p}K_{\mathrm{a,HDIP^+}}\right) + \frac{2.303RT}{F}\mathrm{pH} \tag{8}$$

As shown in **Fig. 4**, the transfer potentials experimentally obtained under the acidic conditions were approximately constant at $\Delta^{\mathrm{w}}_{\mathrm{o}}\phi^{\circ'}_{\mathrm{HDIP^+}} = 0.00$ V, while the transfer potential exhibited a positive shift with a slope of 0.059 V (= 2.303*RT/F*) at pH > 5. These results bear out DIP as a monobasic species. Although a DIP molecule has eight possible protonation sites (nitrogen atoms), a single protonation would only occur within the examined pH range ($0 \le \mathrm{pH} \le 9.5$). According to the semi-empirical quantum calculations, the heat of formation ($\Delta H^{\circ}_{\mathrm{f}}$) for monoprotonation of DIP at a pyrimidine nitrogen is estimated as ca. −58 kJ mol^{-1}, while $\Delta H^{\circ}_{\mathrm{f}}$ for second protonation is much higher value, 828 kJ mol^{-1} [37]. Hence, the additional protonation of HDIP^+ is unrealistic under the present condition and theoretical predictions support our experimental results. The $\left(\mathrm{p}K_{\mathrm{a,HDIP^+}} - \log P_{\mathrm{DIP}}\right)$ value as a fitting parameter was evaluated as 4.52 from Eq. (8) with $\Delta^{\mathrm{w}}_{\mathrm{o}}\phi^{\circ'}_{\mathrm{HDIP^+}} = 0.00$ V and, thus, the $\log P_{\mathrm{DIP}}$ value in the water|DCE system was estimated to be 1.2 by taking a literature value of $\mathrm{p}K_{\mathrm{a,HDIP^+}} = 5.7$ [31]. The experimental values of $\Delta^{\mathrm{w}}_{\mathrm{o}}\phi^{\circ'}$ and log*P* for the

drugs are summarized in **Table 1**. The simple ion transfer features were observed for $HPRO^+$ and WAR^- (Supplementary data: **Fig. S1**). The ionic partition diagram for the PRO system in **Fig. 5a** was analyzed in the same manner as the DIP system from the $\Delta_o^w\phi^{1/2}$ values. The $\Delta_o^w\phi^{\circ'}_{HPRO^+}$ and $\log P_{PRO}$ values were 0.12 V and 3.0, respectively, in good agreement with the literature values [5, 6]. In the WAR system, the ionic partition diagram for a lipophilic acid was obtained as shown in **Fig. 5b**, where the boundary lines for $HWAR_o / WAR_w^-$ and $HWAR_o / WAR_w^-$ are expressed by Eqs. (9) and (10):

$$\mathrm{pH} = \log P_{HWAR} + \mathrm{p}K_{a,HWAR} \tag{9}$$

$$\Delta_o^w\phi = \Delta_o^w\phi^{\circ'}_{WAR^-} - \frac{2.303RT}{F}\left(\log P_{HWAR} + \mathrm{p}K_{a,HWAR}\right) + \frac{2.303RT}{F}\mathrm{pH} \tag{10}$$

$\Delta_o^w\phi^{\circ'}_{WAR^-} = -0.10\,\mathrm{V}$ roughly coincides with the literature value, while the $\log P_{HWAR}$ value estimated as 3.7 by taking $\mathrm{p}K_{a,HWAR} = 5.1$ [38] is relatively larger than the literature value of 2.7 [6]. The disparity in $\log P_{HWAR}$ could result from the specific phase volume ratio of the spectroelectrochemical cell used in this study [36] or the difficulty in determining the precise ion transfer potential of WAR^- in the lower pH region, where the ion transfer peaks were observed at potentials close to the negative edge of the potential window (Supplementary data: **Fig. S1**).

3.2. Voltammetric responses of ionizable drugs affected by the dendrimers

The intermolecular association between the ionizable drugs and the PAMAM dendrimers in the aqueous solution was investigated at various pHs by the UV-Vis absorption and fluorescence spectroscopies. **Fig. 6** shows typical excitation and emission spectra of the aqueous solution of DIP in the absence and presence of the equimolar G3.5 dendrimer. The most abundant DIP species at pH 2.2, $HDIP^+$ was not efficient fluorescent species, while the neutral DIP with poor solubility

in water at pH ≥ 7.2 exhibited strong fluorescence. Taking into account the acidity constants of terminal groups and tertiary amines of the dendrimers [23, 39], the net charges (z) on the G3.5 and G4 PAMAM dendrimers are calculated as $+61 \geq z_{\text{G3.5 PAMAM}} \geq -64$ at $2.1 \leq \text{pH} \leq 9.5$ and $+126 \geq z_{\text{G4 PAMAM}} \geq +2$ at $2.1 \leq \text{pH} \leq 10.6$, respectively. Under the present pH conditions, the spectral profiles of DIP in the aqueous solution were not practically influenced by adding the dendrimers (see also Supplementary data: **Fig. S2** for the G4 PAMAM dendrimer system). In aqueous micellar systems, the DIP species located in a less polar environment such as micellar core indicate the intense fluorescence with a blue-shift of the emission maximum [29, 40]. The present spectral results would be indicative of no efficient interaction between DIP species and the hydrophobic interior of the dendrimers in the bulk aqueous phase. No spectral evidence for the association with the dendrimers were also observed for the PRO and WAR systems. (Supplementary data: **Fig. S3**).

The voltammetric responses in the presence of the equimolar concentration of the drugs and dendrimers were significantly dependent on the pH conditions (**Fig. 7** and Supplementary data: **Fig. S4**). The general features of CVs were analogous to those for the G3.5 and G4 PAMAM dendrimers reported previously [20, 23]. **Fig.7** shows the CVs measured for DIP with the G3.5 PAMAM dendrimer. At pH 2.2, the G3.5 PAMAM dendrimer exists as the cationic species ($z \approx +60$). The positive and negative current peaks observed around 0.35 V and 0.25 V in **Fig. 7a** relate to the ion transfer of the positively charged G3.5 PAMAM dendrimer. The broad voltammetric responses at $0 < \Delta_{\text{o}}^{\text{w}}\phi < 0.20\,\text{V}$ are also associated with the interfacial adsorption of the G3.5 PAMAM dendrimer [23]. In addition, the ion transfer response for HDIP^{+} was observed at around 0 V. At pH 7.2 where the net charges on the dendrimer is ca. −53, the capacitive current was increased in the whole potential region (**Fig. 7b**), indicating the interfacial adsorption of the charged species. Under the alkaline condition at pH 9.5, the G3.5 PAMAM dendrimer showed no

clear voltammetric responses (**Fig. 7c**), nevertheless the ion transfer currents of $HDIP^+$ at around 0.28 V were slightly decreased in the presence of the dendrimer. The similar current decrease was also observed for the cationic PRO system under the neutral and alkaline conditions in the presence of the G3.5 PAMAM dendrimer (**Fig. 8a**). On the other hand, the anionic WAR system showed no clear difference even in the presence of the cationic G4 PAMAM dendrimer with higher positive charges (**Fig. 8b**). These voltammetric results indicate that the ion transfer process of the cationic drugs is certainly affected by the oppositely charged G3.5 PAMAM dendrimer at the polarized interface. The ion transfer potentials and ionic partition diagrams of $HDIP^+$ and $HPRO^+$ were, however, not shifted in the presence of the dendrimers. It has been reported that a multipoint electrostatic interaction of ionic species with the dendrimer significantly enhances the ion association stability whereas a monovalent ion is not appreciably associated with the dendrimer [23, 24]. The ambiguous effects of the dendrimer for the monovalent drug cations could be due to weak interaction with the G3.5 PAMAM dendrimer.

3.3 PMF analysis of interfacial behavior of DIP in the presence of dendrimers

As shown in **Figs. 7** and **8a**, the electrochemical responses associated with the cationic drugs ($HDIP^+$ and $HPRO^+$) were slightly affected by the negatively charged G3.5 PAMAM dendrimer, in which the peak currents under neutral and alkaline conditions decreased in the presence of the dendrimer. Under the acidic condition at pH 2.2 (**Fig. 7a**), the voltammetric responses of DIP were totally buried in those of the dendrimer. In order to study the effect of the dendrimer on the interfacial behavior of cationic drugs in detail, the PMF analysis was carried out for the DIP species which indicates the distinct fluorescence emission in the visible wavelength region. **Fig. 9a** shows the potential dependences of the PMF signal for $HDIP^+$ in the presence and

absence of the equimolar G3.5 PAMAM dendrimer at pH 2.2. The weak real (ΔF_{re}) and imaginary components (ΔF_{im}) were obtained as positive and negative signs around −0.07 V. The PMF signal associated with a quasi-reversible ion transfer (ΔF_t) under the TIR excitation can be expressed as a function of the faradic ac current ($i_{f,ac}$) [34, 35]

$$\Delta F_t = \frac{4.606\varepsilon\Phi_f I_0}{j\omega zFS\cos\Psi} i_{f,ac} \tag{11}$$

where ε is the molar absorption coefficient, Φ_f is the fluorescence quantum yield, I_0 is the excitation light intensity, j is the imaginary number (= $(-1)^{0.5}$), ω is the angular frequency of ac potential modulation, and F is Faraday constant. The real ($\Delta F_{t,re}$) and imaginary components ($\Delta F_{t,im}$) of Eq.(11) are described as:

$$\Delta F_{t,re} = \frac{4.606\varepsilon\Phi_f I_0}{zFS\cos\Psi}\left[\frac{\Delta_o^w\phi_1\sigma\omega^{-3/2}}{\left(R_{ct}+\sigma\omega^{-1/2}\right)^2+\left(\sigma\omega^{-1/2}\right)^2}\right] \tag{12}$$

$$\Delta F_{t,im} = -\frac{4.606\varepsilon\Phi_f I_0}{zFS\cos\Psi}\left[\frac{\Delta_o^w\phi_1\left(R_{ct}+\sigma\omega^{-1/2}\right)\omega^{-1}}{\left(R_{ct}+\sigma\omega^{-1/2}\right)^2+\left(\sigma\omega^{-1/2}\right)^2}\right] \tag{13}$$

where R_{ct}, σ and $\Delta_o^w\phi_1$ are the charge transfer resistance, the Warburg term and the amplitude of ac potential, respectively. It has been established that the real and imaginary components of the PMF signal for an ion transfer of a cationic species across the interface are expressed as positive and negative values at an ion-transfer potential, respectively. The PMF signal at −0.07 V, thus, associates with the transfer process of cationic species, i.e., $HDIP^+$. In addition, the relatively strong PMF signals with the negative ΔF_{re} and positive ΔF_{im} were observed at $0\text{ V} \le \Delta_o^w\phi \le 0.10\text{ V}$. The PMF signal associated with an interfacial adsorption from the organic phase (ΔF_a^o) is expressed as [34, 35]:

$$\Delta F_{\mathrm{a,re}}^{\mathrm{o}} = -\frac{2.303\varepsilon\Phi_{\mathrm{f}} I_0 \Gamma_{\mathrm{s}} SbzF}{RT}\left[\frac{\Delta_{\mathrm{o}}^{\mathrm{w}}\phi_1\left(k_{\mathrm{a},0}\alpha c_0\left(1-\theta_0\right)-k_{\mathrm{d},0}\left(\alpha-1\right)\theta_0\right)\left(k_{\mathrm{a},0}c_0+k_{\mathrm{d},0}\right)}{\left(k_{\mathrm{a},0}c_0+k_{\mathrm{d},0}\right)^2+\omega^2}\right] \quad (14)$$

$$\Delta F_{\mathrm{a,im}}^{\mathrm{o}} = \frac{2.303\varepsilon\Phi_{\mathrm{f}} I_0 \Gamma_{\mathrm{s}} SbzF}{RT}\left[\frac{\Delta_{\mathrm{o}}^{\mathrm{w}}\phi_1\left(k_{\mathrm{a},0}\alpha c_0\left(1-\theta_0\right)-k_{\mathrm{d},0}\left(\alpha-1\right)\theta_0\right)\omega}{\left(k_{\mathrm{a},0}c_0+k_{\mathrm{d},0}\right)^2+\omega^2}\right] \quad (15)$$

where Γ_{s}, b, θ_0, α, $k_{\mathrm{a},0}$, $k_{\mathrm{d},0}$ and c_0 are the saturated surface concentration, the portion of the applied potential employed for the adsorption process (~0.5), the surface coverage, the overall transfer coefficient for the adsorption process, the adsorption and desorption rate constants and the bulk concentration, respectively. The appropriate reverse sign is applied to Eqs. (14) and (15) for the adsorption process from the aqueous phase because of an opposite potential dependence of the surface concentration. The present PMF results demonstrated that $HDIP^+$ is transferred across the interface accompanied by the adsorption process at the organic side of the interface as schematically shown in **Fig. 10**. The PMF responses for the adsorption process of $HDIP^+$ exhibited apparent negative shifts in the presence of the G3.5 PAMAM dendrimer. At pH 2.2, the estimated net charges on the G3.5 PAMAM dendrimer is ca. +60. The strong adsorption of the positively charged G3.5 PAMAM dendrimer at the water|DCE interface has been reported in the positive potential region [23]. The negative shift of the adsorption responses of $HDIP^+$ therefore could result from the electrostatic repulsion by the positively charged dendrimers adsorbed at the interface. On the other hand, the PMF response of the adsorption of $HDIP^+$ was hardly changed in the presence of the G4 PAMAM dendrimer at pH 2.2 (Supplementary data: **Fig. S5a**). As reported previously [24], the interfacial adsorption of the G4 PAMAM dendrimer is observed at $\Delta_{\mathrm{o}}^{\mathrm{w}}\phi > 0.10\ \mathrm{V}$ under acidic conditions, where this potential region is more positive than that of the adsorption of the G3.5 PAMAM dendrimer and $HDIP^+$. Therefore the electrostatic repulsion between $HDIP^+$ and the G4 PAMAM dendrimer seems not to be efficient. In the PMF

measurements, in principle, the interfacial process of only the fluorescence ions is detectable and the interfacial processes associated with non-fluorescent dendrimers should be excluded from the PMF response [20, 32]. The relatively weak PMF signals were, however, observed at $\Delta_o^w\phi > 0.30$ V, where the ion transfer and adsorption of the G3.5 PAMAM dendrimer take place at the water|DCE interface. The PMF responses observed at the positive edge of the potential window agreed with those of the G3.5 PAMAM dendrimer incorporating anilinonaphthalenesulfonates [23]. Taking into account the positive net charges on the dendrimer under acidic conditions, the only neutral DIP can stably be encapsulated into the hydrophobic interior of the dendrimer. The fluorescent DIP-G3.5 PAMAM dendrimer associates are therefore responsible for the PMF signals at $\Delta_o^w\phi > 0.30$ V. At pH 7.2 and 9.5, the neutral DIP was initially dissolved in the organic phase because of the low solubility in water. At pH 7.2, ΔF_{re} and ΔF_{im} were obtained as positive and negative signs around the transfer potential of $HDIP^+$ superimposed on the broad adsorption responses with the opposite sign in the absence of the dendrimer (**Fig. 9b**). The PMF responses for the ion transfer process were broaden at $\Delta_o^w\phi > 0$ V and the adsorption responses of $HDIP^+$ were disappeared by adding the dendrimer in the aqueous phase. The broad PMF responses suggest the complex interfacial process involving the distribution of neutral DIP from the organic phase into the hydrophobic interior of the dendrimers adsorbed at the interface and the protonation of DIP in the aqueous phase (**Fig. 10**). The additional bell-shaped PMF responses around the negative edge of the potential window relate to the adsorption process of the negatively charged dendrimer associated with $HDIP^+$ at the aqueous side of the interface [23]. In the G4 PAMAM dendrimer system (Supplementary data: **Fig. S5b)**, the distorted PMF signals associated with the ion transfer and adsorption of the dendrimer were observed at $\Delta_o^w\phi > 0.30$ V similarly to the G3.5 PAMAM

dendrimer system at pH 2.2. Under alkaline conditions, the 62 tertiary amines and 64 carboxylate groups of the G3.5 PAMAM dendrimer was totally deprotonated and the dendrimer has −64 charges on the periphery moiety. As shown in **Fig. 9c**, the well-defined PMF responses for the transfer of $HDIP^+$ across the interface were observed around 0.26 V both in the absence and presence of the dendrimer at pH 9.5. In addition, the gradual increase of the PMF response at $\Delta_o^w\phi$ > 0.35 V relates to the adsorption process of $HDIP^+$ at the organic side of the interface. The PMF intensities were slightly weakened in the presence of the dendrimer in agreement with the voltammetric features in **Fig. 7c**. These results suggest that the transfer process of $HDIP^+$ was depressed through the intermolecular association between the neutral DIP (or $HDIP^+$) and the hydrophobic interior (or the negatively charged periphery) of the G3.5 PAMAM dendrimer. The PMF signals associated with the transfer process of $HDIP^+$ were also attenuated in the presence of the G4 PAMAM dendrimer under alkaline conditions (Supplementary data: **Fig. S5c**). The hydrophobic interaction between the neutral DIP and the dendrimer is presumed to be the principal effect in the G4 PAMAM dendrimer system. Although the interfacial mechanism of the non-fluorescent PRO species could not be analyzed in detail, the similar attenuation of the ion transfer response in the CVs for $HPRO^+$ might be interpreted as analogous mechanism (**Fig. 8a**).

4. Conclusions

The interfacial behavior of the ionizable drugs in the presence of the PAMAM dendrimers was studied at the polarized water|DCE interface. The intrinsic interfacial mechanism of the ionizable drugs was significantly affected by acid-base equilibrium as well as liquid-liquid distribution of neutral species. The voltammetric results indicated the weak interaction between

the cationic drugs (DIP and PRO) and the dendrimers, while the ion transfer feature of the anionic WAR was hardly changed by adding the dendrimers. The interfacial mechanism of the fluorescent DIP species was analyzed in detail by the PMF spectroscopy. The PMF analysis uncovered the specific interaction between the DIP species and the PAMAM dendrimers only in the interfacial region, albeit with no distinct evidence obtained from the conventional spectral and electrochemical measurements. The interfacial mechanism of the DIP species was significantly changed by adding the dendrimers, in which the pH and potential dependent reactivities of the dendrimers dominantly affected the transfer and adsorption processes of the DIP species through electrostatic repulsion and hydrophobic interaction. The effects of those noncovalent interactions on the interfacial behavior of drugs are adjustable by applying the appropriate potential. The present results demonstrated that the potential ability of the dendrimer as a modifier for the pharmacokinetic properties of drug molecules on a biomembrane. In particular, the membrane permeability and reactivity of ionizable drugs could be affected by the dendrimer. The detailed analysis of the interfacial association of ionizable drugs with the dendrimer at ITIES will contribute to the development of the dendrimer-based DDS with multiple functionalities such as pH- and membrane potential-sensitive drug release and loading.

Acknowledgements

This work was supported by a Grant-in-Aid for Scientific Research (C) (No.24550097) from Japan Society for the Promotion of Science (JSPS) and the Kanazawa University CHOZEN Project. H. S. thanks the JSPS Research Fellowship for Young Scientists (No.15J03765). The authors are grateful for valuable discussions with Dr. Kotaro Morita of Kanazawa University.

References

[1] H.H. Girault, Electrochemistry at Liquid-Liquid Interfaes, in: A.J. Bard (Ed.) Electroanalytical Chemistry: A Series of Advances, CRC Press, 2010, p. 1.

[2] M. Senda, Y. Kubota, H. Katano, Voltammetric study of drugs at liquid-liquid interfaces, in: A.G. Volkov (Ed.) Liquid interfaces in chemical, biological, and pharmaceutical applications, New York, 2001, p. 683.

[3] F. Reymond, Transfer mechanisms and lipophilicity of ionizable drugs, in: A.G. Volkov (Ed.) Liquid interfaces in chemical, biological, and pharmaceutical applications, Marcel Dekker, New York, 2001, p. 729.

[4] F. Reymond, G. Steyaert, P.A. Carrupt, B. Testa, H.H. Girault, Ionic partition diagrams: A Potential pH representation, J. Am. Chem. Soc., 118 (1996) 11951.

[5] M.A. Deryabina, S.H. Hansen, J. Ostergaard, H. Jensen, Effect of α-cyclodextrin on drug distribution studied by electrochemistry at interfaces between immiscible electrolyte solutions, J. Phys. Chem. B, 113 (2009) 7263.

[6] M.A. Deryabina, S.H. Hansen, H. Jensen, Molecular interactions in lipophilic environments studied by electrochemistry at interfaces between immiscible electrolyte solutions, Anal. Chem., 80 (2008) 203.

[7] F. Reymond, V. Chopineaux-Courtois, G. Steyaert, G. Bouchard, P.A. Carrupt, B. Testa, H.H. Girault, Ionic partition diagrams of ionisable drugs: pH-lipophilicity profiles, transfer mechanisms and charge effects on solvation, J. Electroanal. Chem., 462 (1999) 235.

[8] K. Arai, F. Kusu, K. Takamura, Electrochemical behavior of drugs at the oil/water interface, in: A.G. Volkov, D.W. Deamer (Eds.) Liquid-Liquid Interfaces Theory and Methods, CRC Press,

1996, p. 375.

[9] K. Kontturi, L. Murtomaki, Electrochemical determination of partition-coefficients of drugs, J. Pharm. Sci., 81 (1992) 970.

[10] A.K. Kontturi, K. Kontturi, L. Murtomaki, D.J. Schiffrin, An Electrochemical study of long-chain aliphatic-amines, Acta Chem. Scand., 46 (1992) 47.

[11] D.A. Tomalia, J.B. Christensen, U. Boas, Dendrimers, dendrons, and dendritic polymers: discovery, applications, and the future, Cambridge University Press, Cambridge, 2012.

[12] Y.Y. Cheng, L.B. Zhao, Y.W. Li, T.W. Xu, Design of biocompatible dendrimers for cancer diagnosis and therapy: current status and future perspectives, Chem. Soc. Rev., 40 (2011) 2673.

[13] D.A. Tomalia, Dendrons/dendrimers: quantized, nano-element like building blocks for soft-soft and soft-hard nano-compound synthesis, Soft Matter, 6 (2010) 456.

[14] D. Astruc, E. Boisselier, C. Ornelas, Dendrimers designed for functions: From Physical, photophysical, and supramolecular properties to applications in sensing, catalysis, molecular electronics, photonics, and nanomedicine, Chem. Rev., 110 (2010) 1857.

[15] S. Svenson, Dendrimers as versatile platform in drug delivery applications, Eur. J. Pharm. Biopharm., 71 (2009) 445.

[16] Y.Y. Cheng, T.W. Xu, The effect of dendrimers on the pharmacodynamic and pharmacokinetic behaviors of non-covalently or covalently attached drugs, Eur. J. Med. Chem., 43 (2008) 2291.

[17] D.A. Tomalia, Birth of a new macromolecular architecture: dendrimers as quantized building blocks for nanoscale synthetic polymer chemistry, Prog. Polym. Sci., 30 (2005) 294.

[18] E.R. Gillies, J.M.J. Frechet, Dendrimers and dendritic polymers in drug delivery, Drug Discovery Today, 10 (2005) 35.

[19] A. Berduque, M.D. Scanlon, C.J. Collins, D.W.M. Arrigan, Electrochemistry of non-redox-active poly(propylenimine) and poly(amidoamine) dendrimers at liquid-liquid interfaces, Langmuir, 23 (2007) 7356.

[20] H. Nagatani, T. Ueno, T. Sagara, Spectroelectrochemical analysis of ion-transfer and adsorption of the PAMAM dendrimer at a polarized liquid|liquid interface, Electrochim. Acta, 53 (2008) 6428.

[21] M. Calderon, L.M.A. Monzon, M. Martinelli, A.V. Juarez, M.C. Strumia, L.M. Yudi, Electrochemical study of a dendritic family at the water/1,2-dichloroethane interface, Langmuir, 24 (2008) 6343.

[22] G. Herzog, S. Flynn, C. Johnson, D.W.M. Arrigan, Electroanalytical behavior of poly-L-lysine dendrigrafts at the interface between two immiscible electrolyte solutions, Anal. Chem., 84 (2012) 5693.

[23] H. Nagatani, T. Sakamoto, T. Torikai, T. Sagara, Encapsulation of anilinonaphthalenesulfonates in carboxylate-terminated PAMAM dendrimer at the polarized water|1,2-dichloroethane interface, Langmuir, 26 (2010) 17686.

[24] H. Sakae, H. Nagatani, K. Morita, H. Imura, Spectroelectrochemical characterization of dendrimer-porphyrin associates at polarized liquid|liquid interfaces, Langmuir, 30 (2014) 937.

[25] H. Nagatani, H. Sakae, T. Torikai, T. Sagara, H. Imura, Photoinduced electron transfer of PAMAM dendrimer-zinc(II) porphyrin associates at polarized liquidlliquid interfaces, Langmuir, 31 (2015) 6237.

[26] M. Velicky, K.Y. Tam, R.A.W. Dryfe, Hydrodynamic voltammetry at the liquid-liquid interface: Application to the transfer of ionised drug molecules, J. Electroanal. Chem., 683 (2012) 94.

[27] D.R. Shalinsky, A.P. Jekunen, J.E. Alcaraz, R.D. Christen, S. Kim, S. Khatibi, S.B. Howell, Regulation of initial vinblastine influx by P-glycoprotein, Br. J. Cancer, 67 (1993) 30.

[28] E. Bastida, J. del Prado, L. Almirall, G.A. Jamieson, A. Ordinas, Inhibitory effects of dipyridamole on growth, nucleoside incorporation, and platelet-activating capability in the U87MG and SKNMC human tumor cell lines, Cancer Res., 45 (1985) 4048.

[29] N. Karanikolopoulos, M. Zamurovic, M. Pitsikalis, N. Hadjichristidis, Poly(DL-lactide)-b-poly(N,N-dimethylamino-2-ethyl methacrylate): Synthesis, characterization, micellization behavior in aqueous solutions, and encapsulation of the hydrophobic drug dipyridamole, Biomacromolecules, 11 (2010) 430.

[30] M. Tabak, I.E. Borisevitch, Interaction of dipyridamole with micelles of lysophosphatidylcholine and with bovine serum-albumin - Fluorescence studies, Biochim. Biophys. Acta, 1116 (1992) 241.

[31] I.E. Borisevitch, M. Tabak, Electronic absorption and fluorescence spectroscopic studies of dipyridamole-Effects of solution composition, J. Lumin., 51 (1992) 315.

[32] H. Nagatani, T. Sagara, Potential-modulation spectroscopy at solid/liquid and liquid/liquid interfaces, Anal. Sci., 23 (2007) 1041.

[33] T. Wandlowski, V. Mareček, Z. Samec, Galvani potential scales for water-nitrobenzene and water-1,2-dichloroethane interfaces, Electrochim. Acta, 35 (1990) 1173.

[34] H. Nagatani, D.J. Fermín, H.H. Girault, A kinetic model for adsorption and transfer of ionic species at polarized liquid|liquid interfaces as studied by potential modulated fluorescence spectroscopy, J. Phys. Chem. B, 105 (2001) 9463.

[35] H. Nagatani, R.A. Iglesias, D.J. Fermín, P.F. Brevet, H.H. Girault, Adsorption behavior of charged zinc porphyrins at the water/1,2-dichloroethane interface studied by potential modulated

fluorescence spectroscopy, J. Phys. Chem. B, 104 (2000) 6869.

[36] V. Gobry, S. Ulmeanu, F. Reymond, G. Bouchard, P.A. Carrupt, B. Testa, H.H. Girault, Generalization of ionic partition diagrams to lipophilic compounds and to biphasic systems with variable phase volume ratios, J. Am. Chem. Soc., 123 (2001) 10684.

[37] C.N. Alves, M. Castilho, L.H. Mazo, M. Tabak, A.B.F. da Silva, Theoretical calculations on dipyridamole structure allow to explain experimental properties associated to electrochemical oxidation and protonation, Chem. Phys. Lett., 349 (2001) 146.

[38] M. Otagiri, J.G. Fokkens, G.E. Hardee, J.H. Perrin, The interaction of some coumarin anticoagulants with beta-cyclodextrin in phosphate buffers, Pharm. Acta Helv., 53 (1978) 241.

[39] D. Leisner, T. Imae, Polyelectrolyte behavior of an interpolyelectrolyte complex formed in aqueous solution of a charged dendrimer and sodium poly(L-glutamate), J. Phys. Chem. B, 107 (2003) 13158.

[40] P.M. Nassar, L.E. Almeida, M. Tabak, Binding of dipyridamole to DPPG and DPPC phospholipid vesicles: Steady-state fluorescence and fluorescence anisotropy decay studies, Langmuir, 14 (1998) 6811.

Table 1 Formal transfer potentials ($\Delta_o^w\phi^{o'}$) of drug ions and partition coefficients (log*P*) of neutral forms determined by the electrochemical measurements

drug ions	$\Delta_o^w\phi^{o'}$ / V	pK_a	log*P*
$HDIP^+$	0.00	5.7[a]	1.2
$HPRO^+$	0.12 (0.115[b])	9.5[b]	3.0 (3.1[b])
WAR^-	−0.10 (−0.112[b])	5.1[c]	3.7 (2.7[b])

The superscripts *a*, *b* and *c* relate to the literature values in Refs. [31], [6] and [38], respectively.

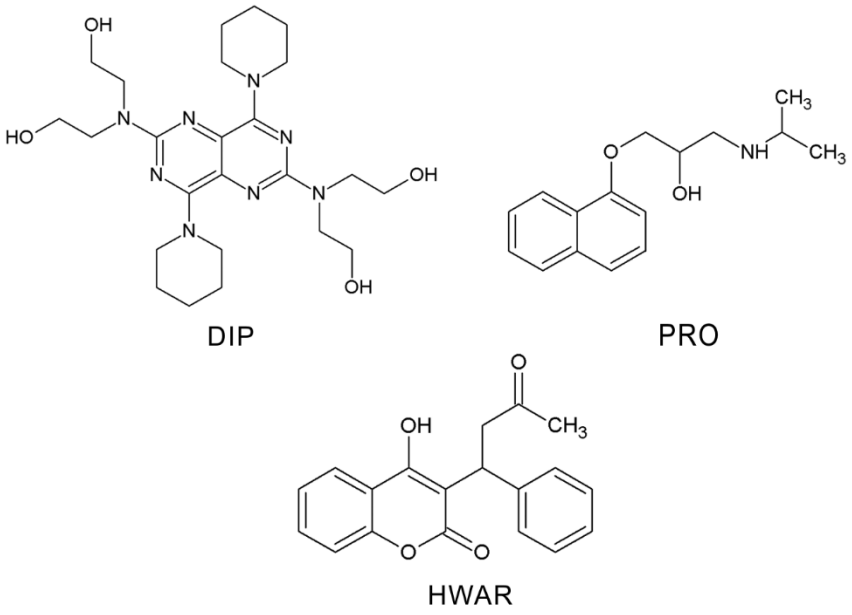

Fig. 1 Molecular structures of dipyridamole (DIP), propranolol (PRO) and warfarin (HWAR).

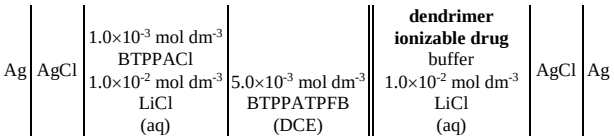

Fig. 2 Composition of the electrochemical cell.

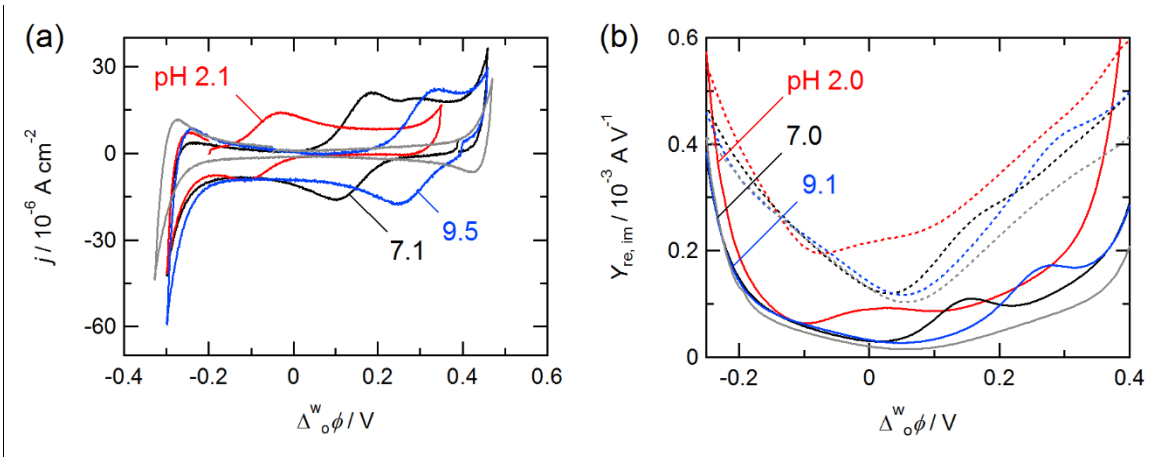

Fig. 3 (a) Cyclic and **(b)** ac voltammograms of DIP measured at the water|DCE interface. **(a)** The gray line refers to CV in the absence of DIP at pH 7.1. The potential sweep rate was 100 mV s^{-1}. The concentration of DIP was 8.0×10^{-5} mol dm^{-3}. **(b)** The solid and dashed lines are the real (Y_{re}) and imaginary (Y_{im}) components of the admittance, respectively. The gray lines refer to the admittance in the absence of DIP at pH 7.1. The potential sweep rate was 5 mV s^{-1}. The amplitude of ac potential modulation was 10 mV at 7 Hz. The concentration of DIP was 1.0×10^{-5} mol dm^{-3}.

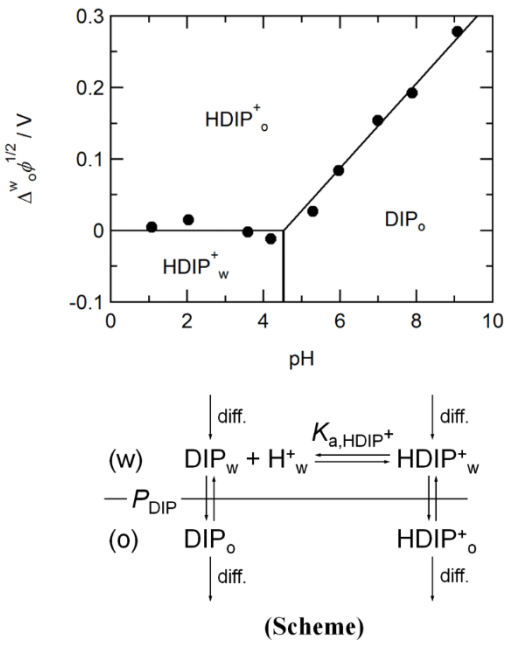

(Scheme)

Fig. 4 Ionic partition diagram for DIP based on the ac voltammograms measured at various pHs. The vertical line represents the estimated value of ($pK_{a,HDIP^+} - \log P_{DIP}$). The concentration of DIP was 1.0×10^{-5} mol dm^{-3}. **(Scheme)** The reaction scheme for the partition of DIP associated with the acid-base equilibrium in the aqueous phase. The subscripts w and o denote the water and organic phases, respectively

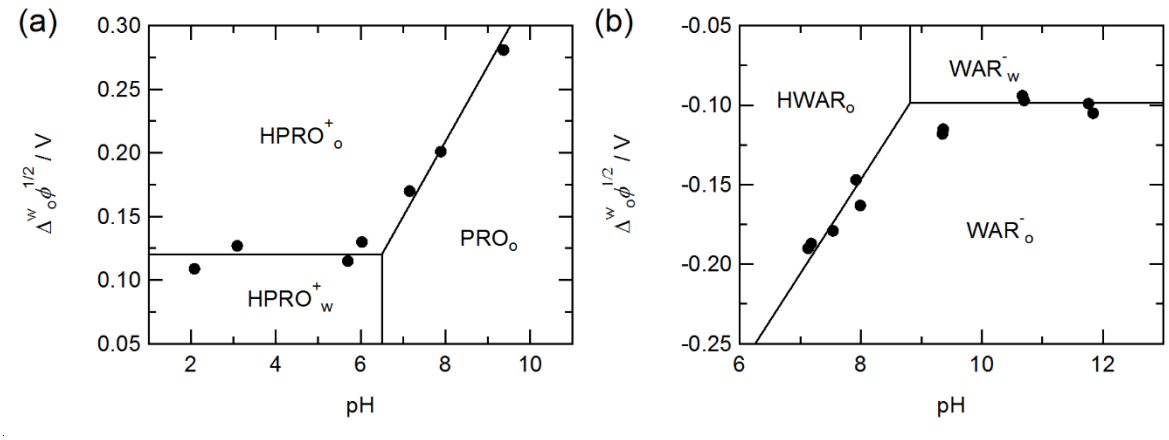

Fig. 5 Ionic partition diagrams for **(a)** PRO and **(b)** WAR based on the voltammograms measured at various pHs. The concentration of PRO and WAR was 1.0×10^{-4} mol dm^{-3}.

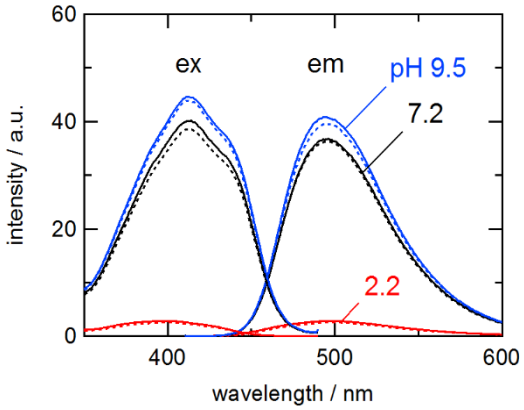

Fig. 6 Excitation and emission spectra of DIP in the aqueous solution at various pHs. The dashed and solid lines refer to spectra in the absence and presence of the equimolar G3.5 PAMAM dendrimer. The concentration of DIP and the dendrimer was 1.0×10^{-5} mol dm^{-3}. The excitation wavelength was 404 nm.

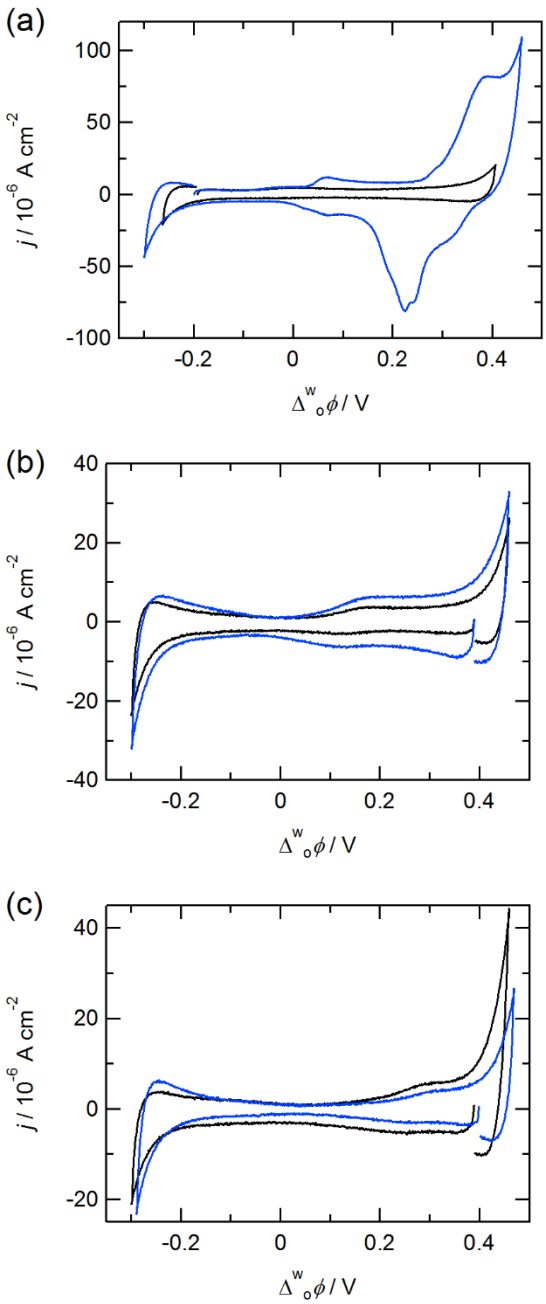

Fig. 7 Cyclic voltammograms measured for DIP at pH **(a)** 2.2, **(b)** 7.2 and **(c)** 9.5 in the presence of the equimolar G3.5 PAMAM dendrimer. The black and blue lines refer to CVs in the absence and presence of the dendrimer. The potential sweep rate was 100 mV s^{-1}. The concentration of DIP and the dendrimer was 1.0×10^{-5} mol dm^{-3}.

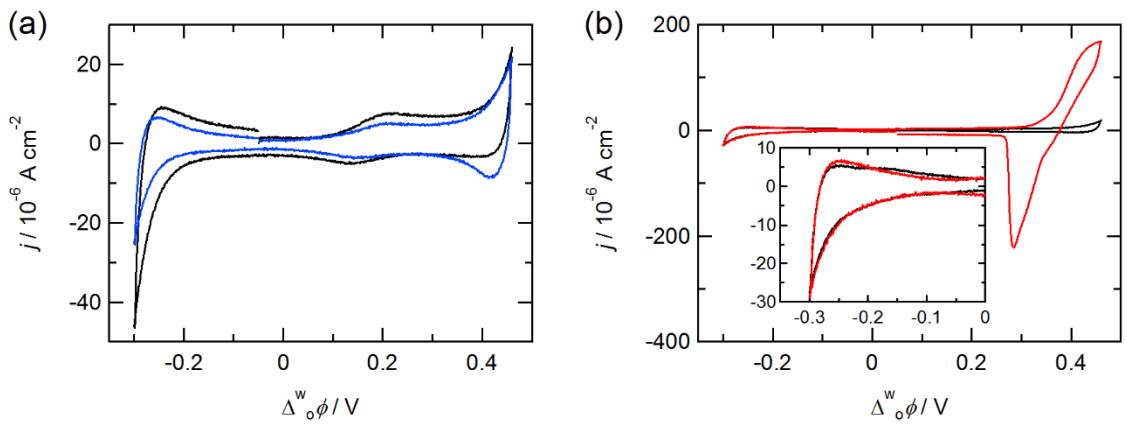

Fig. 8 Cyclic voltammograms measured for **(a)** PRO and **(b)** WAR at pH 7.1. The black lines refer to CVs in the absence of the dendrimers. The blue and red lines refer to CVs in the presence of the G3.5 and G4 PAMAM dendrimers, respectively. The potential sweep rate was 100 mV s^{-1}. The concentration of PRO, WAR and the dendrimers was 2.0×10^{-5} mol dm^{-3}.

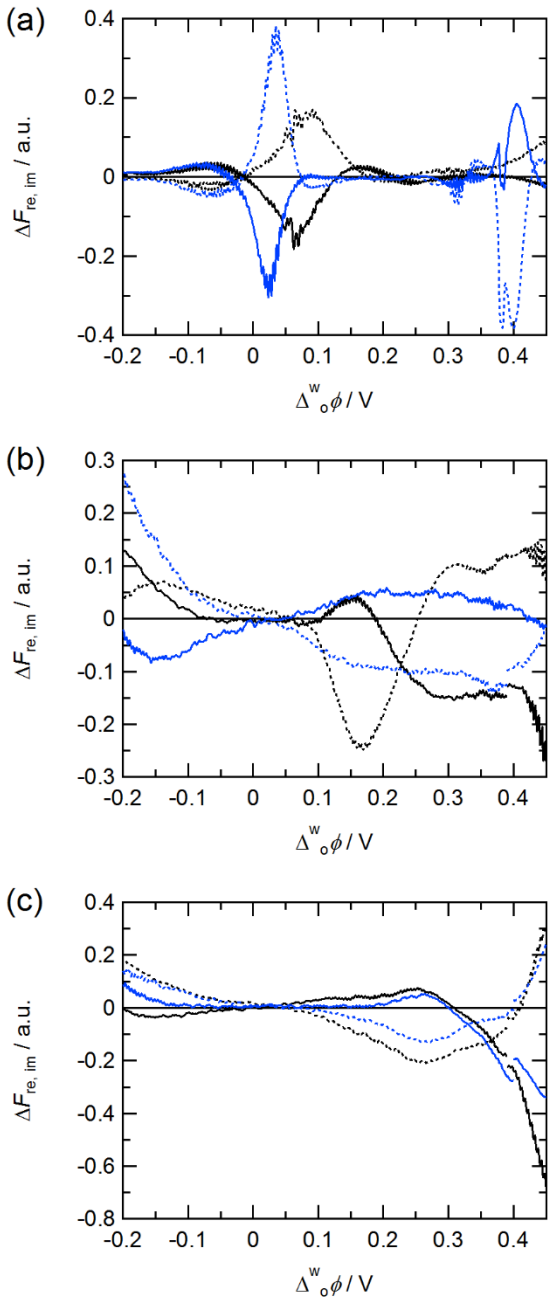

Fig. 9 Potential dependences of the PMF responses measured for DIP at **(a)** pH 2.2, **(b)** 7.2 and **(c)** 9.5. The black and blue lines depict the PMF signals in the absence and presence of the G3.5 PAMAM dendrimer. The solid and dashed lines are the real (ΔF_{re}) and imaginary components (ΔF_{im}), respectively. The potential sweep rate was 5 mV s^{-1}. The amplitudes of ac potential modulation were **(a)** 10 mV and **(b, c)** 20 mV at 1 Hz. The concentration of DIP and the G3.5 PAMAM dendrimer was 1.0×10^{-5} mol dm^{-3}.

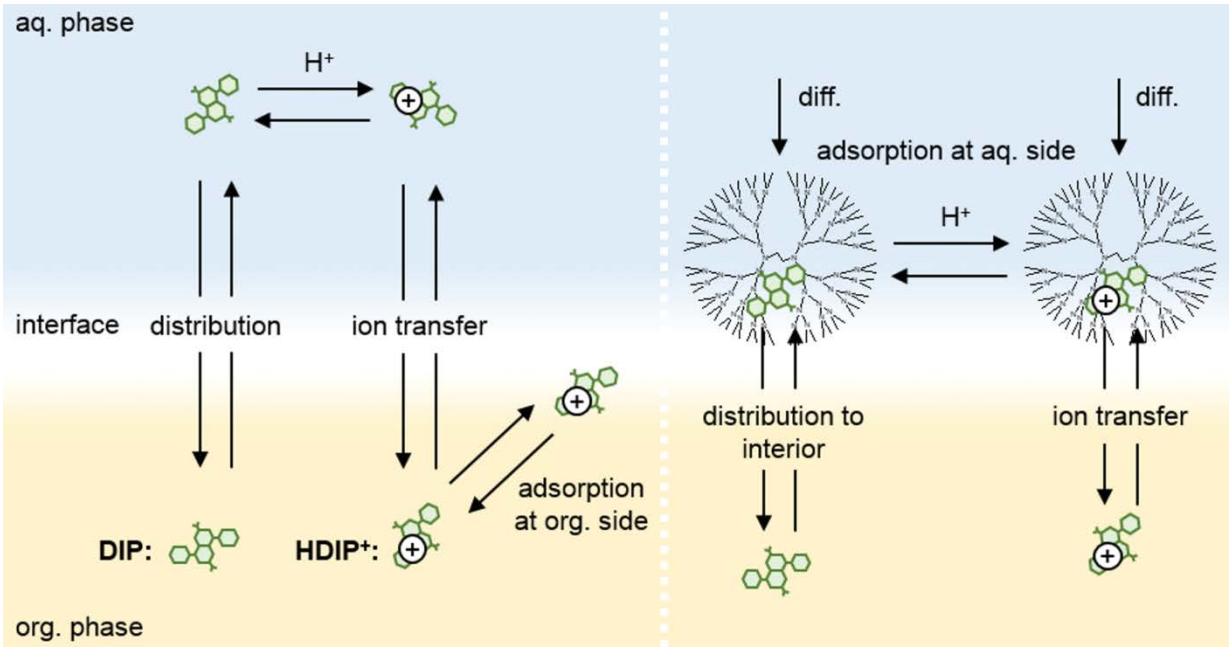

Fig. 10 Schematic representation of the interfacial mechanism of DIP in the absence (left) and presence (right) of the G3.5 PAMAM dendrimer adsorbed at the aqueous side of the interface under neutral conditions.